Draft version October 15, 2019
Preprint typeset using LaTeX style emulateapj v. 08/22/09

MAGNETIC HELICITY DISSIPATION IN AN IDEAL MHD CODE

Axel Brandenburg[1,2,3,4] & Evan Scannapieco[5]
[1]Nordita, KTH Royal Institute of Technology and Stockholm University, Roslagstullsbacken 23, SE-10691 Stockholm, Sweden
[2]Department of Astronomy, AlbaNova University Center, Stockholm University, SE-10691 Stockholm, Sweden
[3]JILA and Laboratory for Atmospheric and Space Physics, University of Colorado, Boulder, CO 80303, USA
[4]McWilliams Center for Cosmology & Department of Physics, Carnegie Mellon University, Pittsburgh, PA 15213, USA
[5]Arizona State University, School of Earth and Space Exploration, P.O. Box 871404, Tempe, AZ 85287, USA
(Dated: Revision: 1.66)
Draft version October 15, 2019

ABSTRACT

We study a turbulent helical dynamo in a periodic domain by solving the ideal magnetohydrodynamic (MHD) equations with the `FLASH` code using the divergence-cleaning eight-wave method and compare our results with with direct numerical simulations (DNS) using the Pencil Code. At low resolution, `FLASH` reproduces the DNS results qualitatively by developing the large-scale magnetic field expected from DNS, but at higher resolution, no large-scale magnetic field is obtained. In all those cases in which a large-scale magnetic field is generated, the ideal MHD equations yield too little power at small scales. As a consequence, the small-scale current helicity is too small compared with the DNS. The resulting net current helicity has then always the wrong sign, and it also does not approach zero at late times, as expected from the DNS. Our results have implications for astrophysical dynamo simulations of stellar and galactic magnetism using ideal MHD codes.

This work was performed at the Aspen Center for Physics, which is supported by National Science Foundation grant PHY-1607611. We enjoyed the stimulating atmosphere during the Aspen program on the Turbulent Life of Cosmic Baryons. This research was supported in part by the Astronomy and Astrophysics Grants Program of the National Science Foundation (grants 1615100 and 1715876).

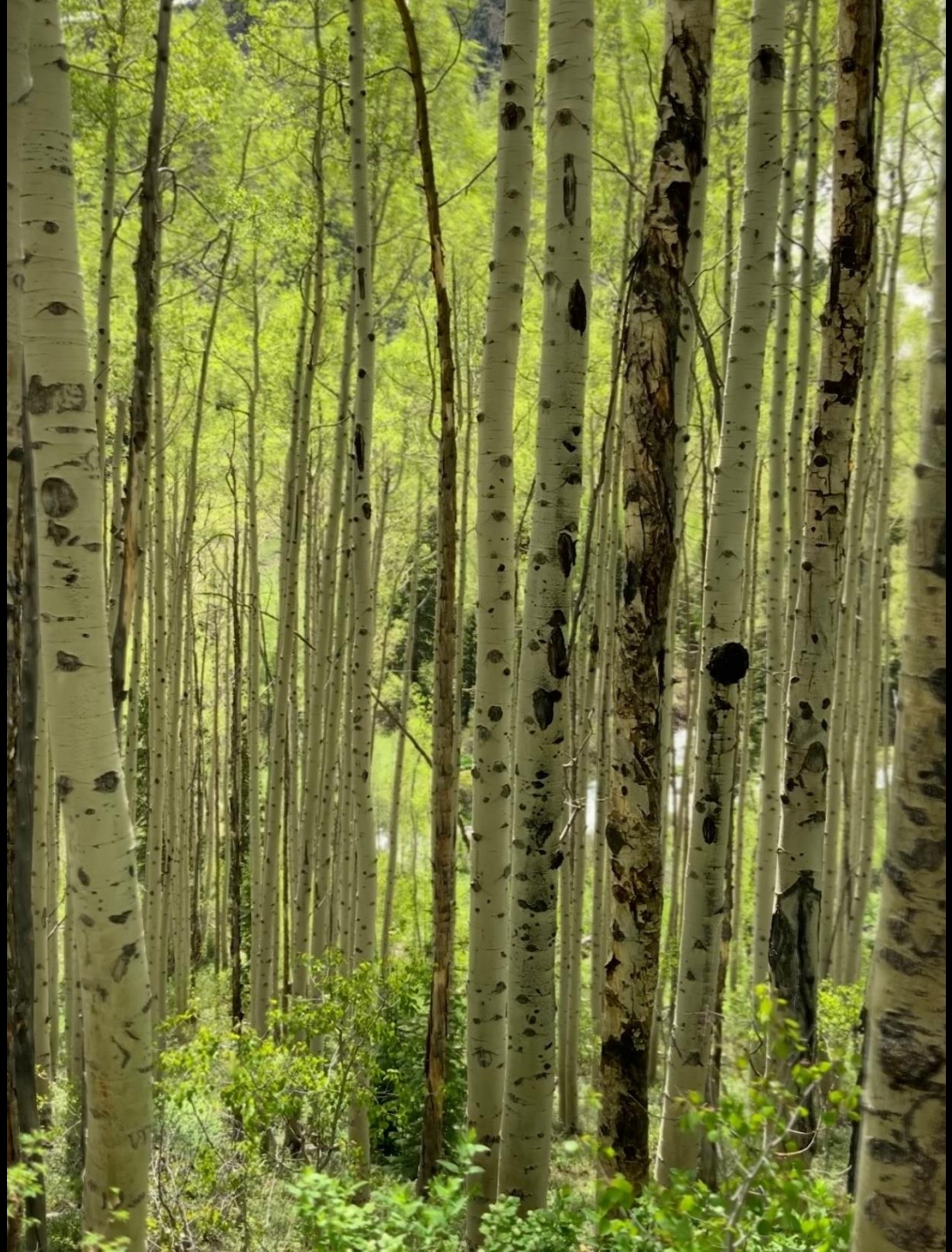

	Title and author(s)	Published in
2019-091	**Magnetic helicity dissipation in an ideal MHD code** *Axel Brandenburg & Evan Scannapieco*	Astrophys. J., submitted (2019)
2019-090	**Small-scale clustering of nano-dust grains in supersonic turbulence** *Lars Mattsson, Johan P. U. Fynbo & Beatriz Villarroel*	MNRAS
2019-089	**X-ray dips and a complex UV/X-ray cross-correlation function in the black hole candidate MAXI J1820+070** *Kajava, J. J. E.; Motta, S. E.; Sanna, A.; Veledina, A.; Del Santo, M.; Segreto, A.*	MNRAS Letters accepted
2019-088	**Pulsating in Unison at Optical and X-Ray Energies: Simultaneous High Time Resolution Observations of the Transitional Millisecond Pulsar PSR J1023+0038** *A. Papitto et al., including A. Veledina*	ApJ
2019-087	**A Black Hole X-ray Binary at 100 Hz: Multiwavelength Timing of MAXI J1820+070 with HiPERCAM and NICER** *J. A. Paice et al., including A. Veledina*	MNRASL
2019-086	**Autoignition and detonation development from a hot spot inside a closed chamber: effects of end wall reflection** *Peng Dai, Zheng Chen, Xiaohua Gan, Mikhail A. Liberman*	
2019-083	**Gravitational waves from first order cosmological phase transitions in the Sound Shell Model** *Mark Hindmarsh and Mulham Hijazi*	
2019-074	**Datasets for ``Spectral magnetic helicity of solar active regions between 2006 and 2017** *Gosain, S., & Brandenburg, A.*	Zenodo, DOI:10.5281/zenodo.3338302
2019-069	**Super-Eddington accretion discs with advection and outflows around magnetized neutron stars** *A. Chashkina, G. Lipunova, P. Abolmasov, J. Poutanen*	Astronomy and Astrophysics, 626, A18 (2019)

MNRAS 000, 1–11 (2019) Preprint 17 October 2019 Compiled using MNRAS LATEX style file v3.0

Small-scale clustering of nano-dust grains in supersonic turbulence

L. Mattsson[1]★, J. P. U. Fynbo[2,3], B. Villarroel[1,4]

[1]Nordita, KTH Royal Institute of Technology and Stockholm University, Roslagstullsbacken 23, SE-106 91 Stockholm, Sweden
[2]The Cosmic Dawn Center (DAWN)
[3]Niels Bohr Institute, Lyngbyvej 2, DK-2100 Copenhagen, Denmark
[4]Instituto de Astrofísica de Canarias (IAC), E-38200 La Laguna, Tenerife, Spain

17 October 2019

ABSTRACT

We investigate the clustering and dynamics of nano-sized particles (nano-dust) in high-resolution (1024^3) simulations of compressible isothermal hydrodynamic turbulence. It is well-established that large grains will decouple from a turbulent gas flow, while small grains will tend to trace the motion of the gas. We demonstrate that nano-sized grains may cluster in a turbulent flow (fractal small-scale clustering), which increases the local grain density by at least a factor of a few. In combination with the fact that nano-dust grains may be abundant in general, and the increased interaction rate due to turbulent motions, aggregation involving nano dust may have a rather high probability. Small-scale clustering will also affect extinction properties. As an example we present an extinction model based on silicates, graphite and metallic iron, assuming strong clustering of grain sizes in the nanometre range, could explain the extreme and rapidly varying ultraviolet extinction in the host of GRB 140506A.

Key words: ISM: dust, extinction – ISM: clouds – turbulence – hydrodynamics

1 INTRODUCTION

Nano-sized dust grains, like graphitic particles, polycyclic aromatic hydrocarbons (PAHs) or even nano diamonds, are by number the

fluid mechanics and statistical physics. For incompressible flows, numerous studies have shown that centrifuging of particles away from vortex cores leads to accumulation of particles in conver-

2019-068	**Properties of the transient X-ray pulsars Swift J1816.7-1613 and its optical companion** *A. Nabizadeh, S.S. Tsygankov, D.I. Karasev, J. Mönkkönen, A.A. Lutovinov, D.I. Nagirner, J. Poutanen*	Astronomy and Astrophysics, 622, A198 (2019)
2019-067	**Evidence for the radiation-pressure dominated accretion disk in bursting pulsar GRO J1744-28 using timing analysis** *J. Mönkkönen, S.S. Tsygankov, A.A. Mushtukov, V. Doroshenko, V.F. Suleimanov, J.Poutanen*	Astronomy and Astrophysics, 626, A106 (2019)
2019-066	**Effects of Compton scattering on the neutron star radius constraints in rotation-powered millisecond pulsars** *Tuomo Salmi, Valery F. Suleimanov, Juri Poutanen*	Astronomy and Astrophysics, 627, A39 (2019)
2019-065	**Generation of a large-scale vorticity in a fast rotating density stratified turbulence or turbulent convection** *Igor Rogachevskii, Nathan Kleeorin*	
2019-061	**Runko: Modern multi-physics toolbox for simulating plasma** *J. Nättilä*	Runko: Modern multi-physics toolbox for simulating plasma
2019-060	**Paleo-Detectors for Galactic Supernova Neutrinos** *Sebastian Baum, Thomas D. P. Edwards, Bradley J. Kavanagh, Patrick Stengel, Andrzej K. Drukier, Katherine Freese, Maciej Górski, Christoph Weniger*	
2019-059	**Kinetics and clustering of dust particles in supersonic turbulence with self-gravity** *Robert Hedvall, Lars Mattsson*	RNAAS
2019-058	**A global two-scale helicity proxy from π-ambiguous solar magnetic fields** *Axel Brandenburg*	Astrophys. J. 883, 119 (2019)
2019-057	**STROBE-X: X-ray Timing and Spectroscopy on Dynamical Timescales from Microseconds to Years** *P. Ray et al., including A. Veledina*	submitted to NASA for Astro2020 Decadal Survey

2019-055	**Pulsar wind-heated accretion disk and the origin of modes in transitional millisecond pulsar PSR J1023+0038** *Alexandra Veledina, Joonas Nättilä, and Andrei M. Beloborodov*	ApJ submitted
2019-054	**Cosmology in f(Q) geometry** *Jose Beltran Jimenez, Lavinia Heisenberg, Tomi Koivisto*	
2019-049	**A First Look on 3D Effects in Open Axion Haloscopes** *Stefan Knirck, Jan Schütte-Engel, Alexander J. Millar, Javier Redondo, Olaf Reimann, Andreas Ringwald, Frank D. Steffen*	
2019-048	**Noether symmetries in Symmetric Teleparallel Cosmology** *Konstantinos F. Dialektopoulos, Tomi S. Koivisto, Salvatore Capozziello*	
2019-046	**Exploring helical dynamos with machine learning** *F. Nauman and J. Nättilä*	
2019-044	**Efficient quasi-kinematic large-scale dynamo as the small-scale dynamo saturates** *Pallavi Bhat, Kandaswamy Subramanian, Axel Brandenburg*	Phys. Rev. Lett., submitted
2019-042	**Testing the rotational nature of the supermassive object M87* from the circularity and size of its first image** *Cosimo Bambi, Katherine Freese, Sunny Vagnozzi, Luca Visinelli*	
2019-041	**Scale-dependent galaxy bias, CMB lensing-galaxy cross-correlation, and neutrino masses** *Elena Giusarma, Sunny Vagnozzi, Shirley Ho, Simone Ferraro, Katherine Freese, Rocky Kamen-Rubio, Kam-Biu Luk*	Phys. Rev. D 98 (2018) 123526
2019-031	**Constraining the properties of neutron-star matter with observations** *Eemeli Annala, Tyler Gorda, Aleksi Kurkela, Joonas Nättilä, Aleksi Vuorinen*	
2019-029	**Reversed dynamo at small scales and large magnetic Prandtl number** *Axel Brandenburg, Matthias Rempel*	Astrophys. J., 879, 57 (2019)

2019-027	**The geometrical trinity of gravity** *Jose Beltran Jimenez, Lavinia Heisenberg, Tomi Koivisto*	
2019-026	**Quark-matter cores in neutron stars** *Eemeli Annala, Tyler Gorda, Aleksi Kurkela, Joonas Nättilä, Aleksi Vuorinen*	
2019-025	**Ambipolar diffusion in large Prandtl number turbulence** *Axel Brandenburg*	Mon. Not. Roy. Astron. Soc. 487, 2673-2684 (2019)
2019-024	**Numerical Simulations of Gravitational Waves from Early-Universe Turbulence** *Roper Pol, A., Mandal, S., Brandenburg, A., Kahniashvili, T., Kosowsky, A.*	Phys. Rev. Lett., submitted
2019-023	**The limited roles of autocatalysis and enantiomeric cross inhibition in achieving homochirality in dilute systems** *Axel Brandenburg*	Orig. Life Evol. Biosph. (submitted)
2019-022	**Butterfly in a Cocoon, Understanding the origin and morphology of Globular Cluster Streams: The case of GD-1** *Khyati Malhan, Rodrigo A. Ibata, Raymond G. Carlberg, Monica Valluri, Katherine Freese*	
2019-021	**Cosmic-Ray Propagation in Light of Recent Observation of Geminga** *G. Johannesson, T. A. Porter, I. V. Moskalenko*	
2019-020	**Unresolved Gamma-Ray Sky through its Angular Power Spectrum** *Fermi-LAT collaboration, including G. Johannesson*	Physical Review Letters, Volume 121, Issue 24, id.241101
2019-019	**A gamma-ray determination of the Universe's star formation history** *Fermi-LAT collaboration, including G. Johannesson*	Science, Volume 362, Issue 6418, pp. 1031-1034 (2018)
2019-018	**MAGIC and Fermi-LAT gamma-ray results on unassociated HAWC sources** *Fermi-LAT collaboration, including G. Johannesson, HAWC collaboration, and MAGIC collaboration.*	Monthly Notices of the Royal Astronomical Society, Volume 485, Issue 1, p.356-366

MHD module & forcing

We use the MHD eight-wave module of FLASH (Derigs et al. 2016), which is based on a divergence-cleaning algorithm. The forcing function is analogous to that used by Sur et al. (2014), except that here only one sign of helicity is used. In particular, we used an artificial forcing term F which is modeled as a stochastic Ornstein-Uhlenbeck process (Eswaran & Pope 1988; Benzi et al. 2008) with a user-specified forcing correlation time, which was taken to be one half. In the following, we consider two values for the scale separation ratio k_f/k_1: a smaller one with a combination of 76 wavevectors with wavenumbers between 2 and 3, and a larger one with 156 wavevectors with wavenumbers between 4 and 5. These cases are distinguished by their average nominal forcing wavenumbers of 2.5 and 4.5, respectively.

Contents lists available at ScienceDirect

Journal of Computational Physics

www.elsevier.com/locate/jcp

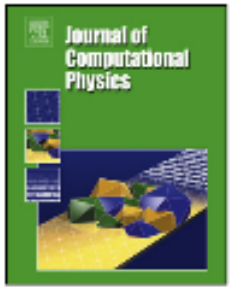

A novel high-order, entropy stable, 3D AMR MHD solver with guaranteed positive pressure

Dominik Derigs [a,*], Andrew R. Winters [b], Gregor J. Gassner [b], Stefanie Walch [a]

[a] I. Physikalisches Institut, Universität zu Köln, Zülpicher Straße 77, 50937 Köln, Germany
[b] Mathematisches Institut, Universität zu Köln, Weyertal 86-90, 50931 Köln, Germany

ARTICLE INFO

Article history:
Received 21 January 2016
Received in revised form 11 April 2016
Accepted 24 April 2016
Available online 28 April 2016

Keywords:
Magnetohydrodynamics
FLASH
Entropy stable
Finite volume schemes
Pressure positivity

ABSTRACT

We describe a high-order numerical magnetohydrodynamics (MHD) solver built upon a novel non-linear entropy stable numerical flux function that supports eight travelling wave solutions. By construction the solver conserves mass, momentum, and energy and is entropy stable. The method is designed to treat the divergence-free constraint on the magnetic field in a similar fashion to a hyperbolic divergence cleaning technique. The solver described herein is especially well-suited for flows involving strong discontinuities. Furthermore, we present a new formulation to guarantee positivity of the pressure. We present the underlying theory and implementation of the new solver into the multi-physics, multi-scale adaptive mesh refinement (AMR) simulation code FLASH (http://flash.uchicago.edu). The accuracy, robustness and computational efficiency is demonstrated with a number of tests, including comparisons to available MHD implementations in FLASH.

Exponential growth + saturation

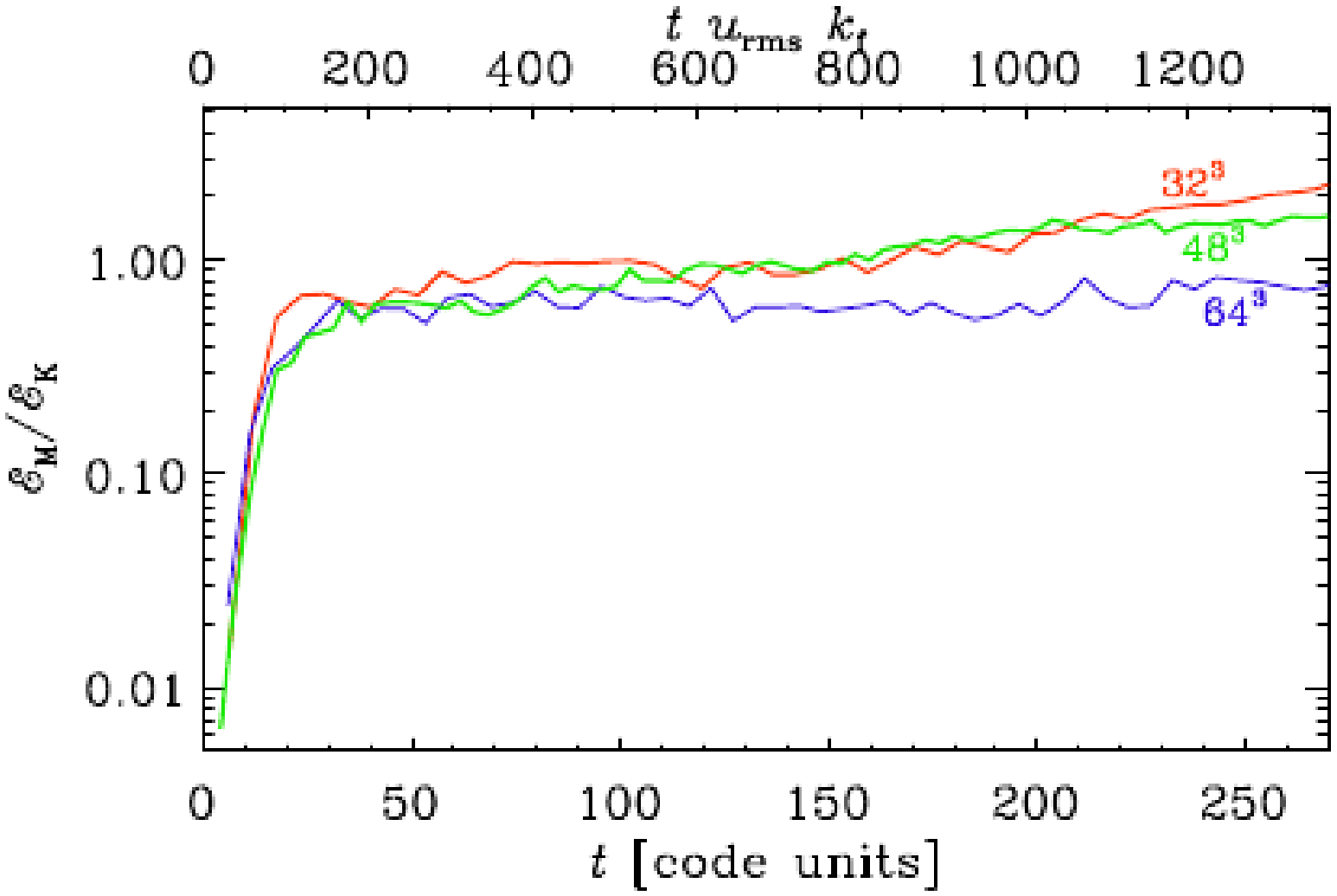

Linear scale, late times

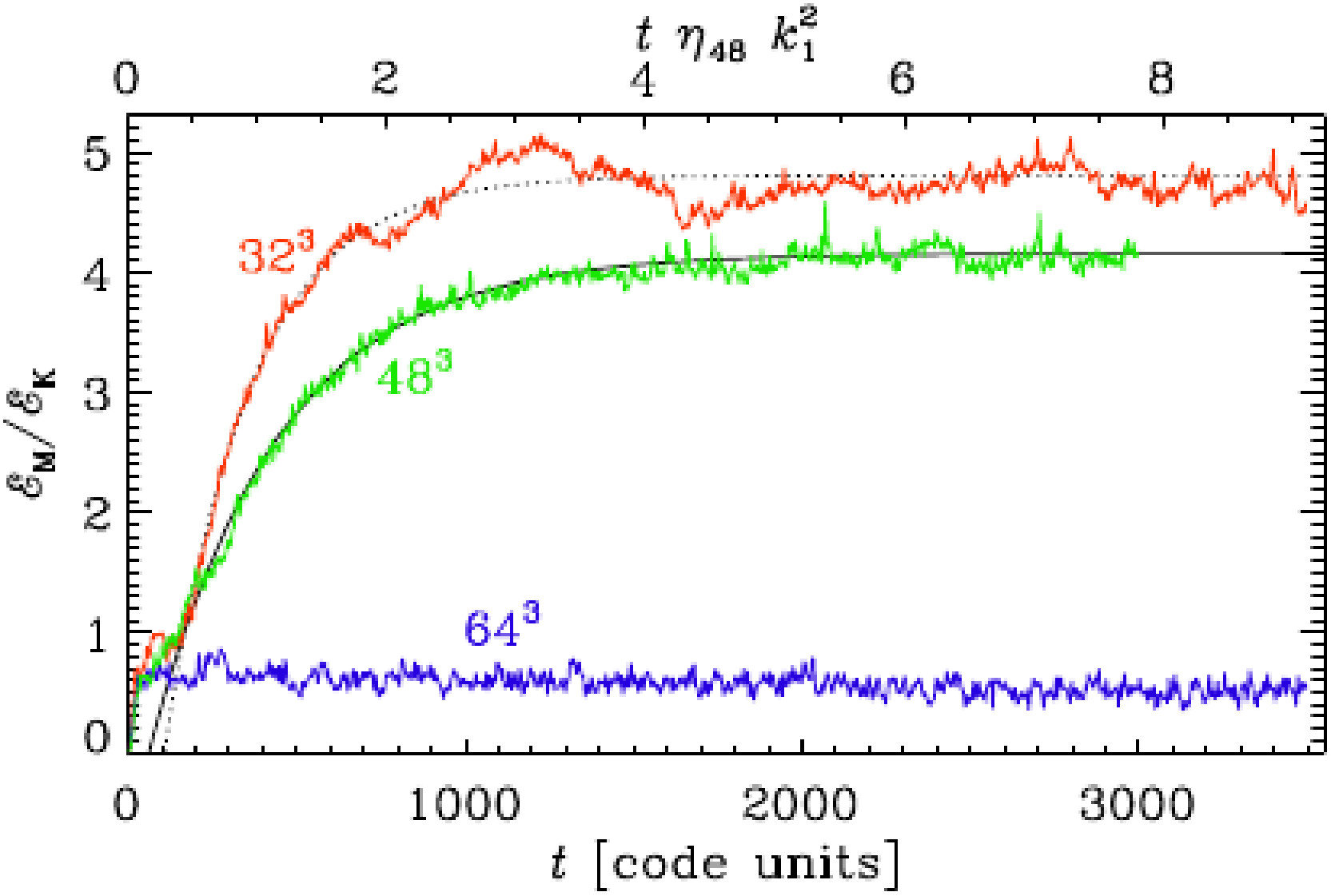

B_x and B_y phase shifted

$$\overline{\boldsymbol{B}} = (\cos k_1 z, \sin k_1 z, 0).$$

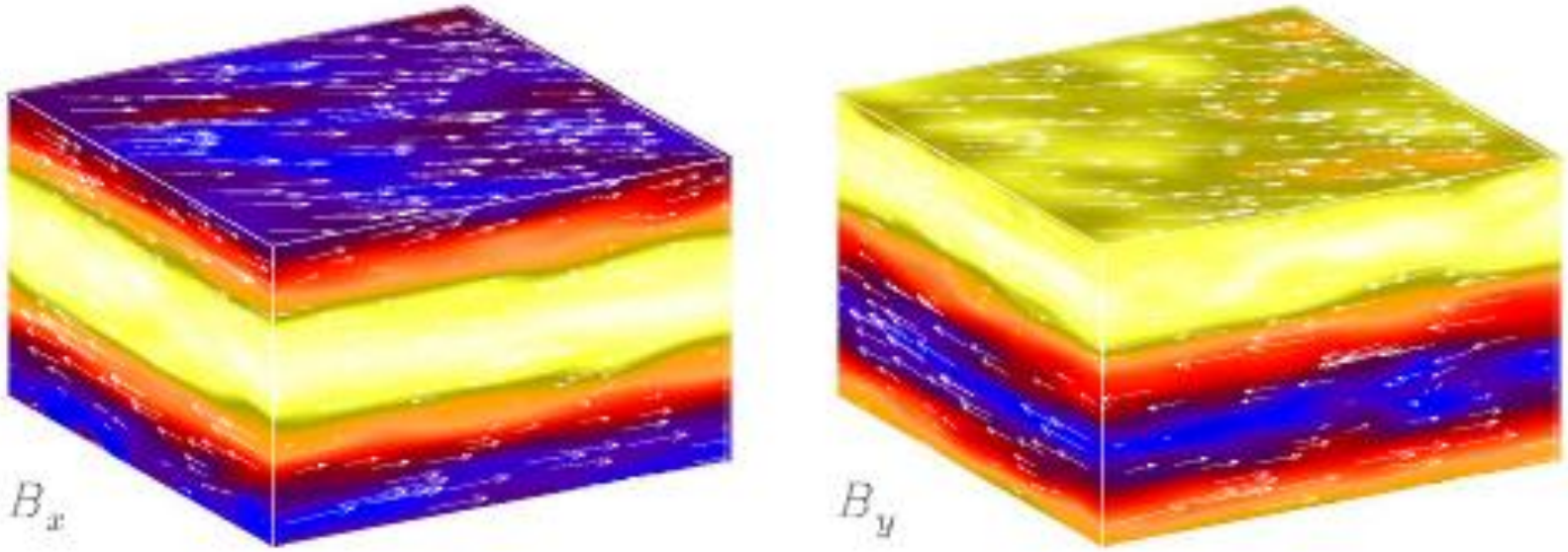

FIG. 10.— B_x and B_y at time 200 (in code units) for $k_f/k_1 = 4.5$. Note that the fields now vary with z, and that the phases of B_x and B_y are shifted by 90° relative to each other. Yellow (blue) shades denote positive (negative) values.

Controlled by magnetic helicity

the current helicity. The evolution of magnetic helicity is then given by

$$\frac{\mathrm{d}}{\mathrm{d}t}\langle \boldsymbol{A}\cdot\boldsymbol{B}\rangle = -2\eta\langle \boldsymbol{J}\cdot\boldsymbol{B}\rangle, \qquad (1)$$

where $\boldsymbol{B} = \boldsymbol{\nabla}\times\boldsymbol{A}$ is the magnetic field in terms of the magnetic vector potential $\boldsymbol{A}$, and $\boldsymbol{J} = \boldsymbol{\nabla}\times\boldsymbol{B}$ is proportional to the current density. As can be seen from Equa-

Expected saturation behavior

Following Brandenburg (2001), we fit the late-time evolution of the magnetic energy to a curve of the form

$$\mathcal{E}_{\rm M}-\mathcal{E}_{\rm K} \approx \mathcal{E}_{\rm K}\,\frac{k_{\rm f}^{\rm eff}}{k_1}\left[1-e^{-2\eta k_1^2(t-t_{\rm sat})}\right] \quad \text{for } t>t_{\rm sat}, \quad (2)$$

where $k_{\rm f}^{\rm eff}$ and $t_{\rm sat}$ are fit parameters that characterize the effective forcing wavenumber and the effective saturation time, respectively (see Appendix A for a derivation).

A. LATE SATURATION PHASE

To understand the origin of Equation (2), we use Equation (1), introduce mean fields, $\overline{\boldsymbol{B}}$, as suitably defined planar averages, and define fluctuations correspondingly as $\boldsymbol{b}=\boldsymbol{B}-\overline{\boldsymbol{B}}$, and likewise for the magnetic vector potential $\boldsymbol{a}=\boldsymbol{A}-\overline{\boldsymbol{A}}$ and the magnetic current density $\boldsymbol{j}=\boldsymbol{J}-\overline{\boldsymbol{J}}$, respectively Equation (1) then becomes

$$\frac{\rm d}{{\rm d}t}\langle\overline{\boldsymbol{A}}\cdot\overline{\boldsymbol{B}}\rangle=-2\eta\langle\overline{\boldsymbol{J}}\cdot\overline{\boldsymbol{B}}\rangle-2\eta\langle\boldsymbol{j}\cdot\boldsymbol{b}\rangle, \quad (A1)$$

where we have ignored the time derivative of $\langle\boldsymbol{a}\cdot\boldsymbol{b}\rangle$, because the small-scale magnetic field has saturated at $t=t_{\rm sat}$; (Figure 1) is approximately constant during the late saturation phase, $t>t_{\rm sat}$. Next, we approximate $\langle\overline{\boldsymbol{A}}\cdot\overline{\boldsymbol{B}}\rangle\approx-\langle\overline{\boldsymbol{B}}^2\rangle/k_1$, $\langle\overline{\boldsymbol{J}}\cdot\overline{\boldsymbol{B}}\rangle\approx-\langle\overline{\boldsymbol{B}}^2\rangle k_1$, and $\langle\boldsymbol{j}\cdot\boldsymbol{b}\rangle\approx+\langle\boldsymbol{b}^2\rangle k_{\rm f}^{\rm eff}$. Finally, we approximate $\langle\boldsymbol{b}^2\rangle/8\pi\approx\mathcal{E}_{\rm K}$, and obtain

$$\left(2\eta k_1^2+\frac{\rm d}{{\rm d}t}\right)\mathcal{E}_{\rm M}=2\eta k_1 k_{\rm f}^{\rm eff}\mathcal{E}_{\rm K}, \quad (A2)$$

which can be integrated to yield Equation (2).

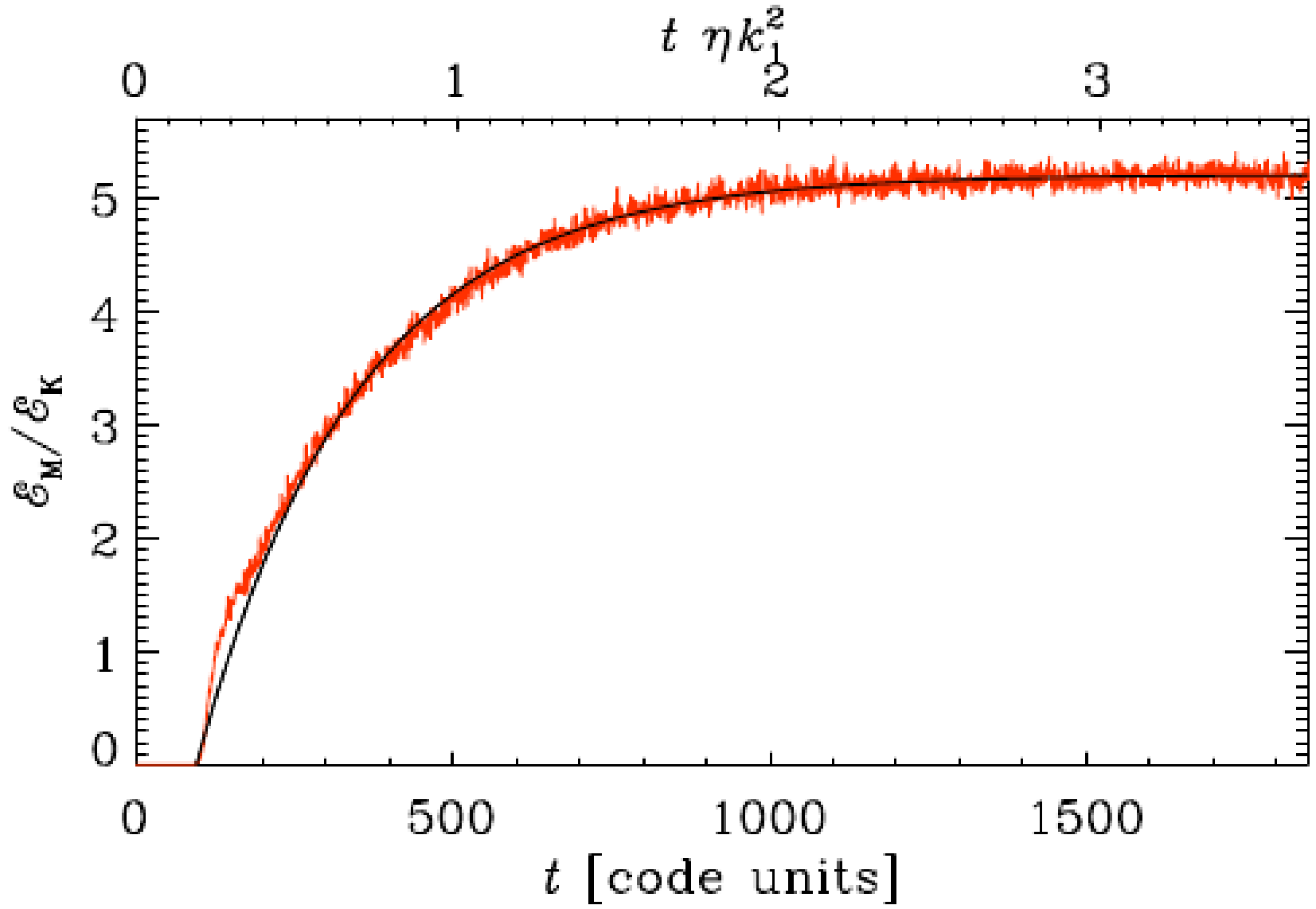

FIG. 12.— Direct numerical simulations with the PENCIL CODE using $\eta = 5 \times 10^{-5}$ and $k_f/k_1 = 4.5$.

TABLE 1
PARAMETERS OF THE VARIOUS RUNS.

Res	$k_{\rm f}$	$u_{\rm rms}$	$k_{\rm f}^{\rm eff}$	$t_{\rm sat}$	η_{-6}	$\eta_{-6}^{\rm eff}$	$3\eta_{\rm t0}/\eta^{\rm eff}$
32^3	2.5	0.28	3.8	170	0	50	360
48^3	2.5	0.30	3.2	170	0	66	270
64^3	2.5	0.30	—	—	0	—	—
64^3	2.5	0.25	11.7	5	5	34	470
32^3	4.5	0.28	8.0	60	0	100	150
48^3	4.5	0.29	—	—	0	—	—
64^3	4.5	0.30	—	—	0	—	—
64^3	4.5	0.25	12.1	5	5	64	140
64^3	4.5	0.21	4.7	10	50	150	49

All quantities are in code units; η_{-6} and $\eta_{-6}^{\rm eff}$ denote values in units of 10^{-6}.

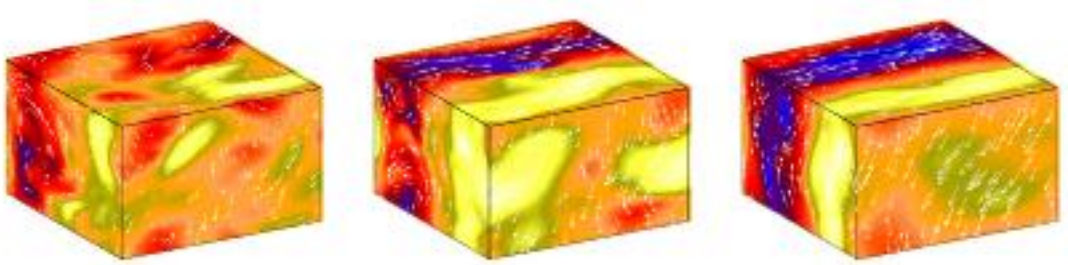

Large scales for 32^3 – not 64^3

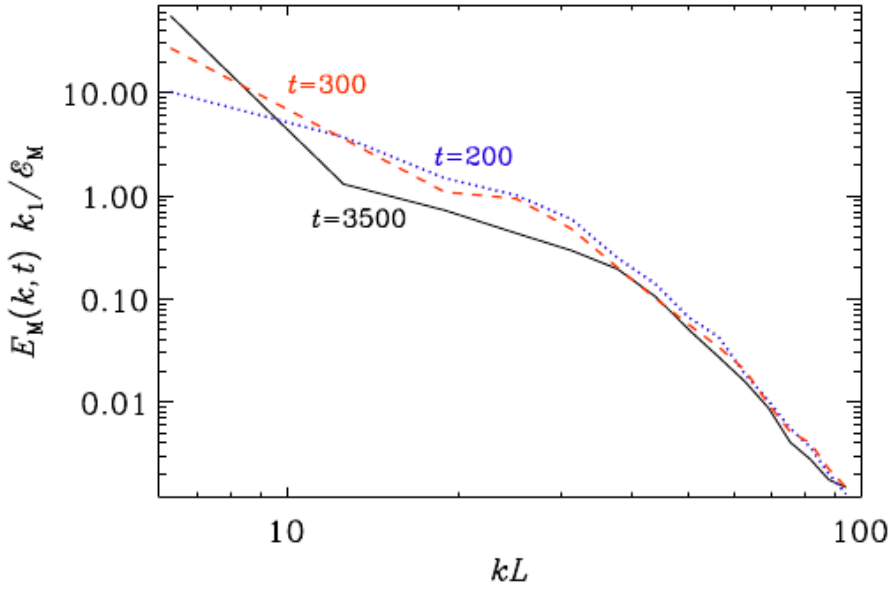

FIG. 4.— Magnetic energy spectra at times 200, 300, and 3500.

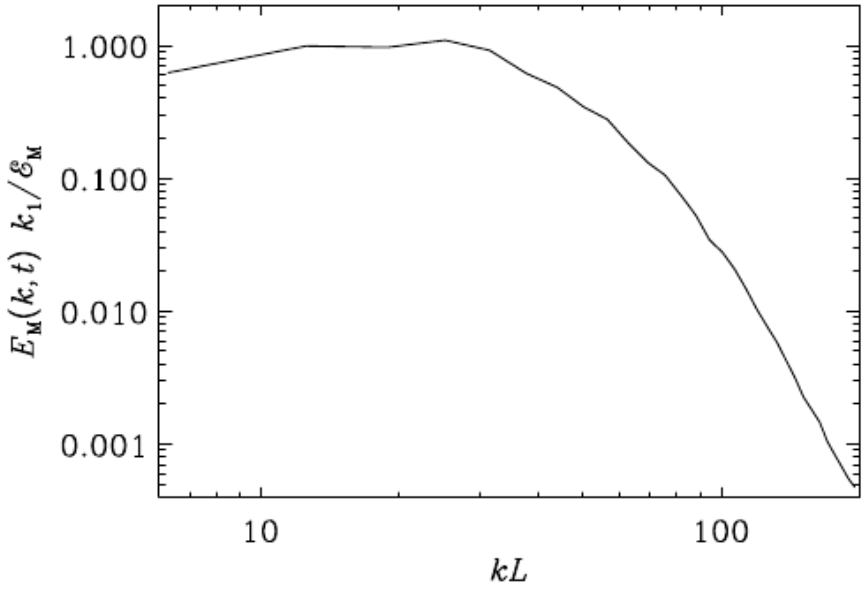

FIG. 6.— Spectra for the higher resolution run with 64^3 mesh points at time 3500, i.e., the end of the run.

Energy & helicity spectra

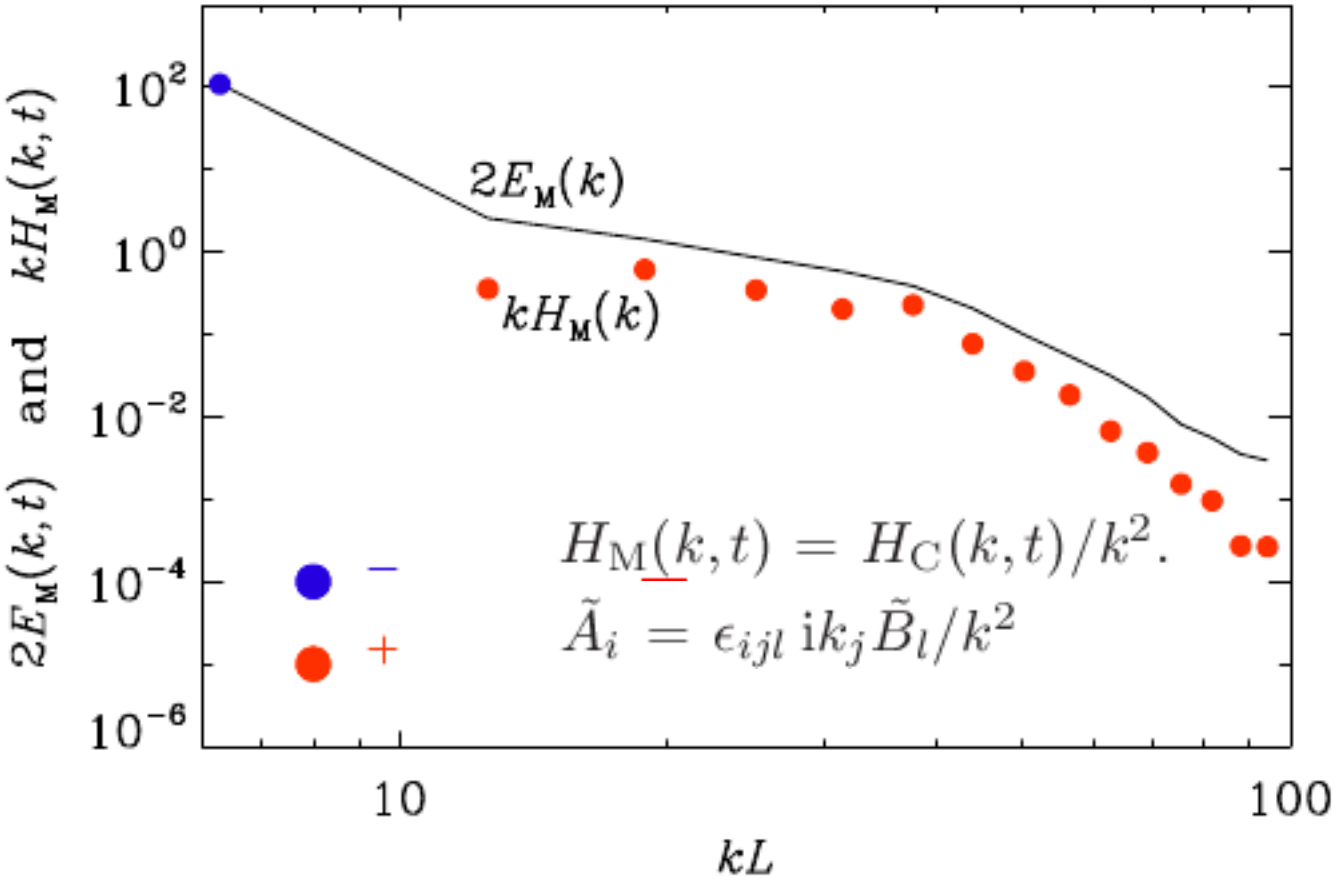

FIG. 9.— Comparison of magnetic energy and helicity spectra for the run with 32^3 mesh points and $k_{\rm f}/k_1 = 2.5$ at $t = 3500$. Positive (negative) values of $H_{\rm M}$ are plotted as red (blue) symbols.

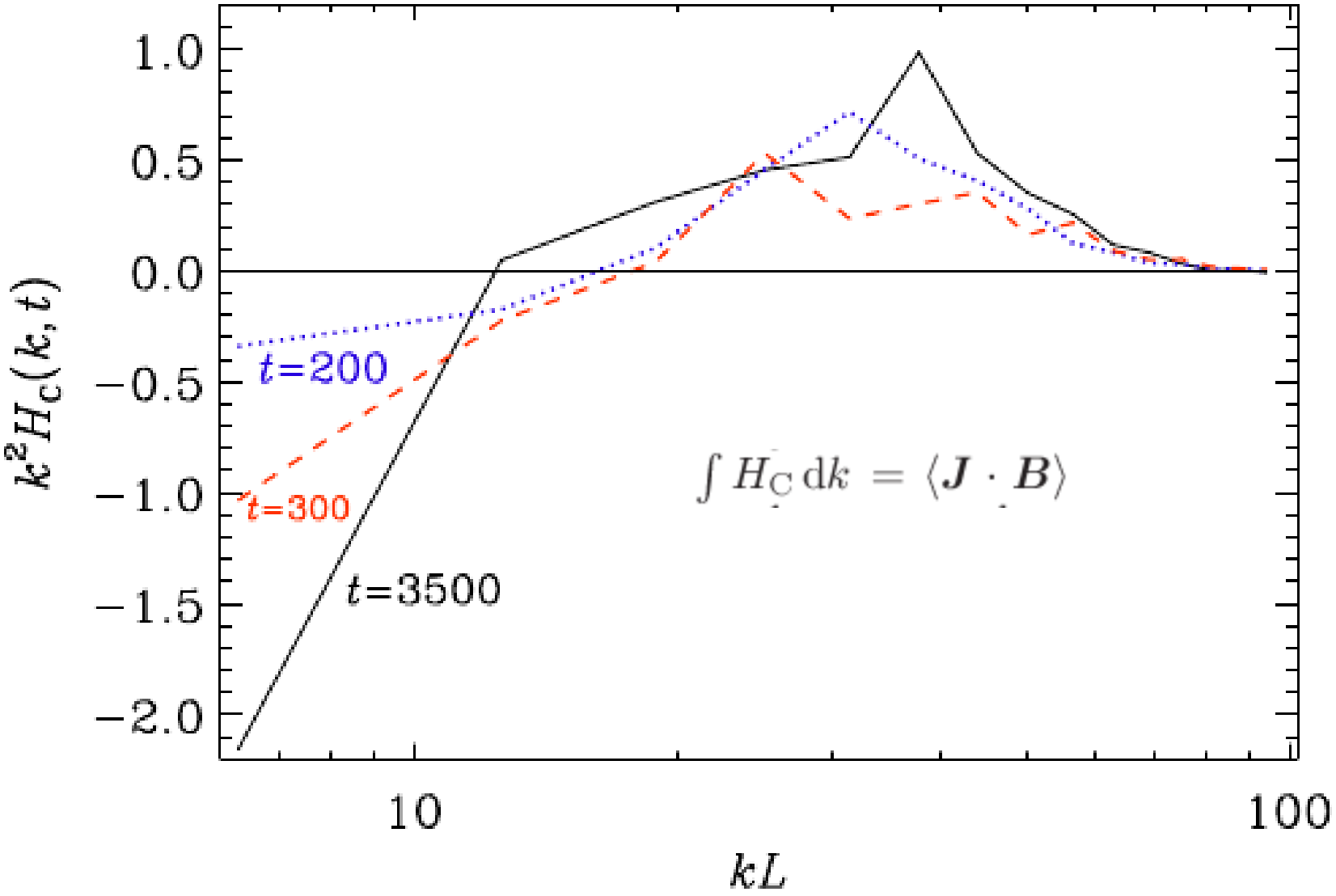

FIG. 5.— Current helicity dissipation spectra, $k^2 H_C(k,t)$, at times 200, 300, and 3500.

Weird oscillation: never seen before

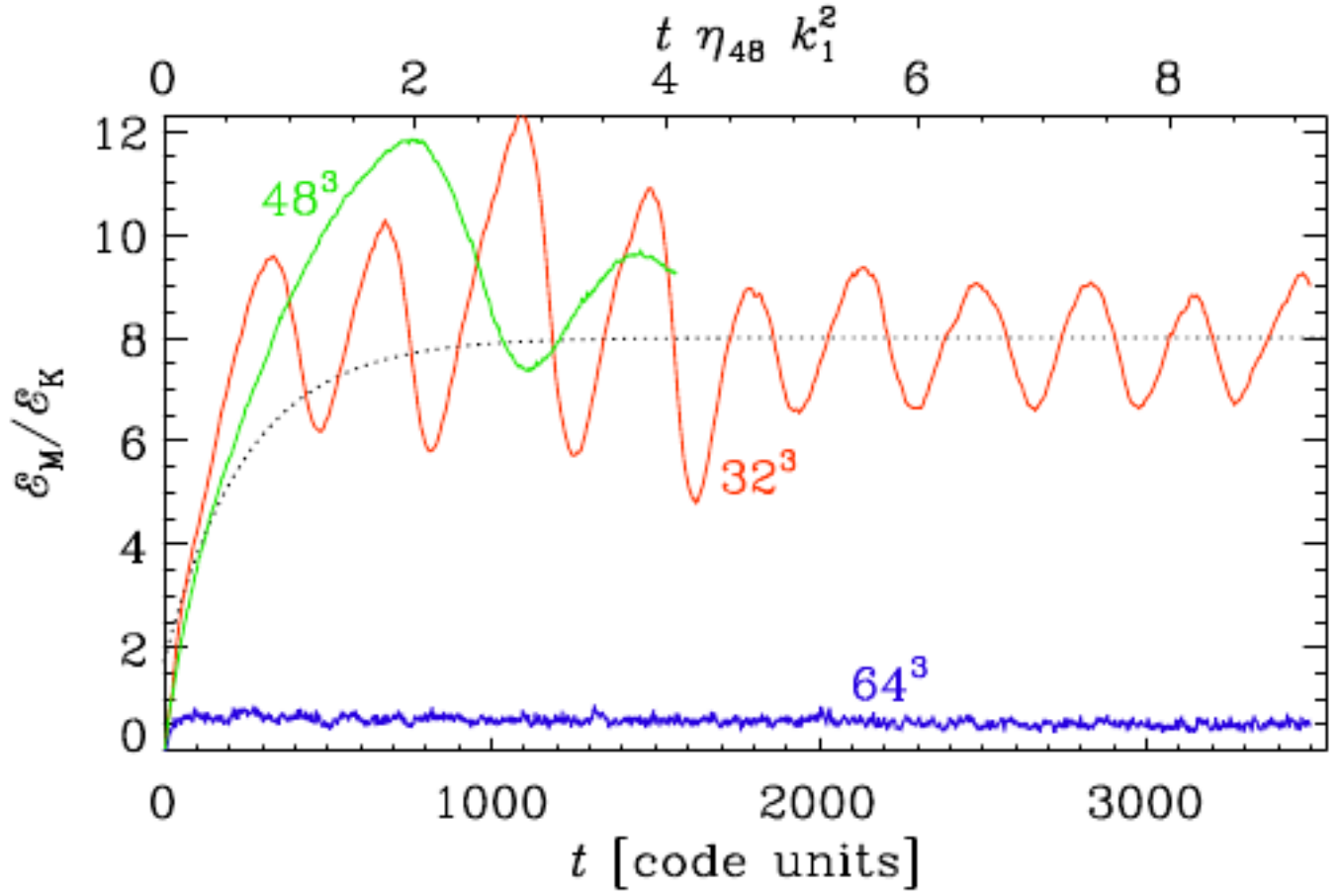

FIG. 7.— Late saturation for resolutions 32^3, 48^3, 64^3 and $k_f/k_1 = 4.5$. The upper abscissa gives time in microphysical diffusion times based on the empirical value η_{48} found for the run with 48^3 mesh points.

Current helicity not zero

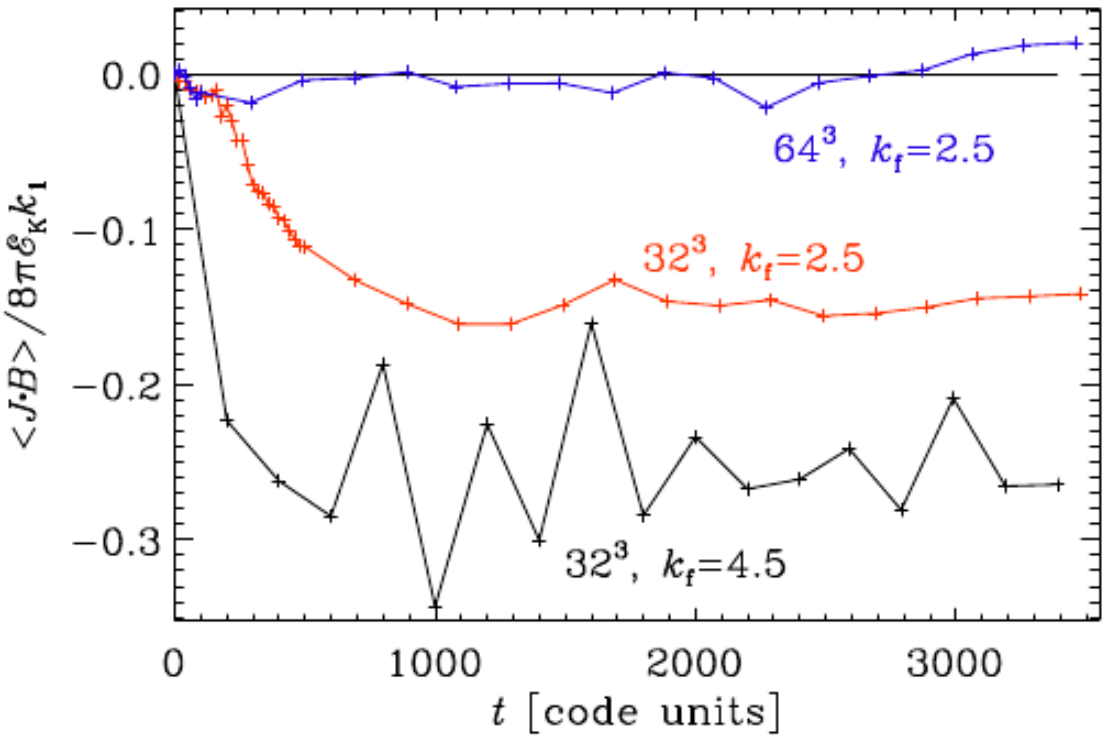

FIG. 8.— Evolution of current helicity for runs with different resolutions (32^3, 64^3) and different scale separation ($k_f/k_1 = 2.5$ and 4.5).

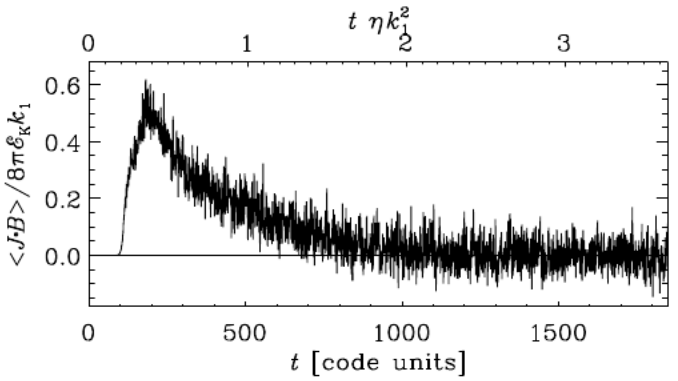

FIG. 13.— Evolution of $\langle \boldsymbol{J} \cdot \boldsymbol{B} \rangle$ for the run of Figure 12

the current helicity. The evolution of magnetic helicity is then given by

$$\frac{\mathrm{d}}{\mathrm{d}t}\langle \boldsymbol{A} \cdot \boldsymbol{B} \rangle = -2\eta \langle \boldsymbol{J} \cdot \boldsymbol{B} \rangle, \qquad (1)$$

where $\boldsymbol{B} = \boldsymbol{\nabla} \times \boldsymbol{A}$ is the magnetic field in terms of the magnetic vector potential $\boldsymbol{A}$, and $\boldsymbol{J} = \boldsymbol{\nabla} \times \boldsymbol{B}$ is proportional to the current density. As can be seen from Equa-

Magnetic helicity at early times

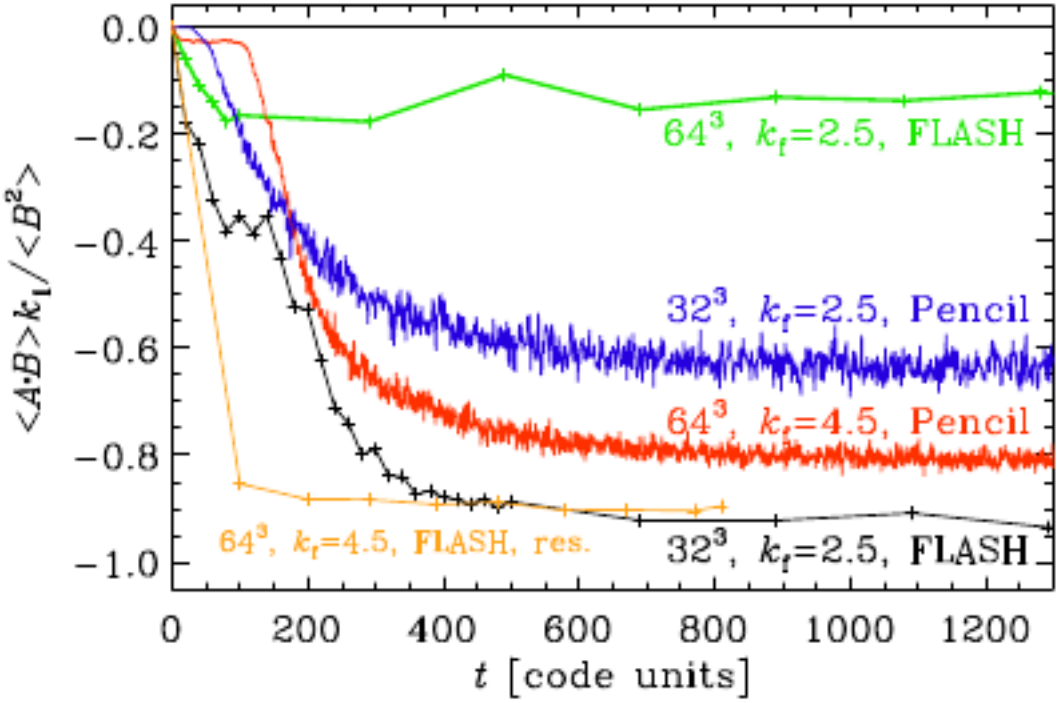

FIG. 14.— Evolution of the fractional magnetic helicity for the case with 32^3 mesh points, $k_f/k_1 = 2.5$, and $\eta^{\rm eff} = 5 \times 10^{-5}$ (black line), compared with the evolution in DNS with 32^3 mesh points, $k_f/k_1 = 2.5$, and $\eta = 5 \times 10^{-5}$ (blue). Also shown are a DNS with 64^3 mesh points ($k_f/k_1 = 4.5$, $\eta = 5 \times 10^{-5}$, red line), and a solution with FLASH with explicit resistivity ($k_f/k_1 = 4.5$, $\eta = 5 \times 10^{-5}$, orange line).

With explicit diffusivity

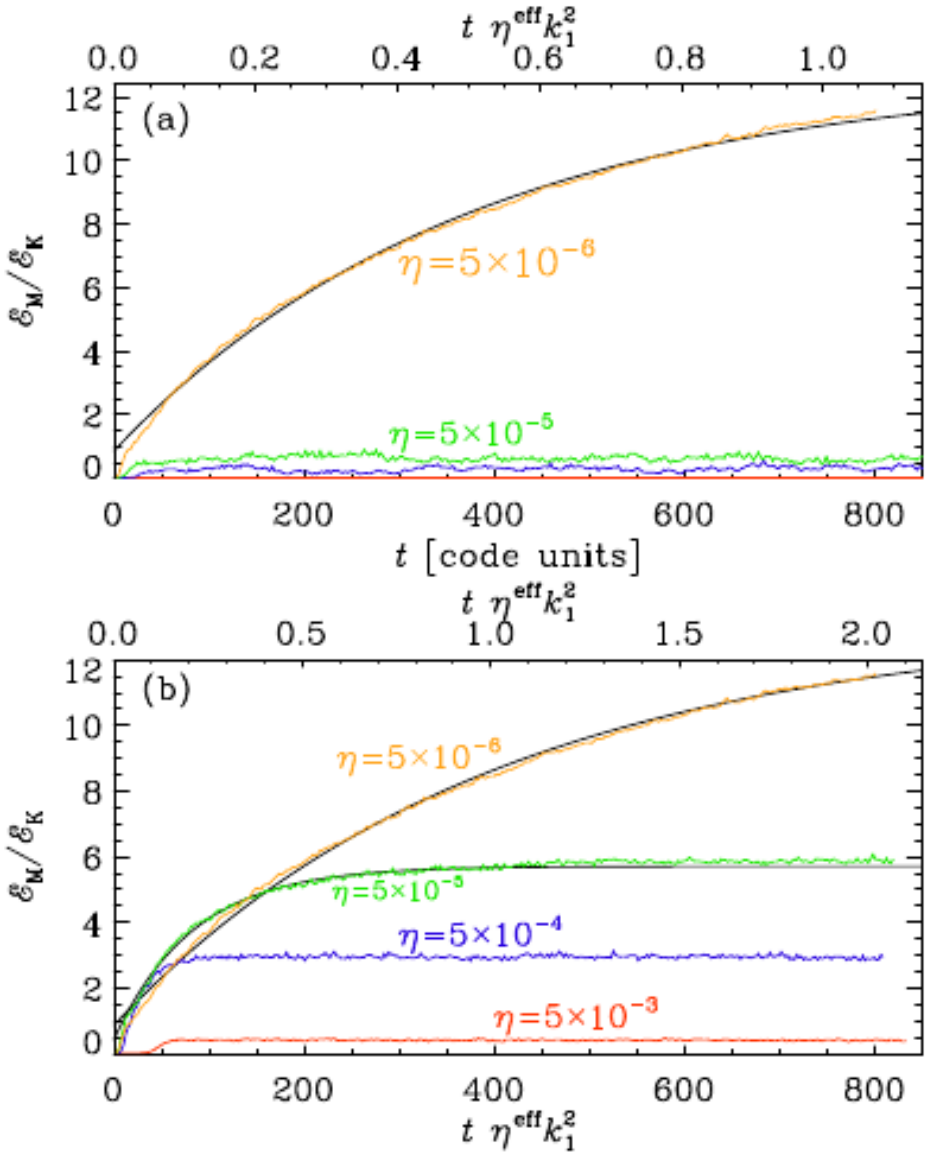

FIG. 11.— Saturation for runs with explicit magnetic diffusivity using (a) $k_{\rm f}/k_1 = 2.5$ and (b) $k_{\rm f}/k_1 = 4.5$ with $\eta = 5\times10^{-3}$ (red), 5×10^{-4} (blue), 5×10^{-5} (green), and 5×10^{-5} (orange), all at a resolution of 64^3 mesh points. The upper abscissa gives time in effective microphysical diffusion times based on the runs with the largest saturation value.

PARAMETERS OF RUNS WITH THE PENCIL CODE.

Res	$k_{\rm f}$	$\mathrm{Pr_M}$	$u_{\rm rms}$	$k_{\rm f}^{\rm eff}$	$t_{\rm sat}$	$3\eta_{\rm t0}/\eta$
32^3	2.2	10	0.11	1.40	120	81
32^3	2.6	10	0.11	1.76	110	81
32^3	4.5	10	0.11	3.20	70	78
64^3	4.5	10	0.12	3.86	90	82
64^3	4.5	20	0.10	4.15	105	70
64^3	4.5	40	0.08	4.20	150	55

cases, $\eta^{\rm eff} = \eta = 5\times10^{-5}$, and $\mathrm{Re_M} = 3\eta_{\rm t0}/\eta$.

Conclusions

- Dynamo in FLASH qualitatively ok
  - But not (at all) quantitatively
- Magnetic helicity violation even at early times
  - So this was independent of Spitzer
- Resolution usually much higher,
  - But then also more structure
  - Which are then effectively still poorly resolved